Author Manuscript

Author Manuscript

Author Manuscript

Author Manuscript

HHS Public Access

Author manuscript

Nature. Author manuscript; available in PMC 2014 July 02.

Published in final edited form as:

Nature. 2014 January 2; 505(7481): 117–120. doi:10.1038/nature12730.

m^{6}A-dependent regulation of messenger RNA stability

Xiao Wang[1], **Zhike Lu**[1], **Adrian Gomez**[1], **Gary C. Hon**[2], **Yanan Yue**[1], **Dali Han**[1], **Ye Fu**[1], **Marc Parisien**[3], **Qing Dai**[1], **Guifang Jia**[1,4], **Bing Ren**[2], **Tao Pan**[3], and **Chuan He**[1,*]

[1]Department of Chemistry and Institute for Biophysical Dynamics, The University of Chicago, 929 East 57th Street, Chicago, Illinois, 60637, USA

[2]Ludwig Institute for Cancer Research, Department of Cellular and Molecular Medicine, UCSD Moores Cancer Center and Institute of Genome Medicine, University of California, San Diego School of Medicine, 9500 Gilman Drive, La Jolla, CA 92093-0653, USA

[3]Department of Biochemistry and Molecular Biology and Institute for Biophysical Dynamics, The University of Chicago, 929 East 57th Street, Chicago, Illinois, 60637, USA

[4]Department of Chemical Biology and Synthetic and Functional Biomolecules Center, College of Chemistry and Molecular Engineering, Peking University, Beijing, China

Abstract

N^6-methyladenosine (m^{6}A) is the most prevalent internal (non-cap) modification present in the messenger RNA (mRNA) of all higher eukaryotes[1,2]. Although essential to cell viability and development[3–5], the exact role of m^{6}A modification remains to be determined. The recent discovery of two m^{6}A demethylases in mammalian cells highlighted the importance of m^{6}A in basic biological functions and disease[6–8]. Here we show that m^{6}A is selectively recognized by the human YTH domain family 2 (YTHDF2) protein to regulate mRNA degradation. We identified over 3,000 cellular RNA targets of YTHDF2, most of which are mRNAs, but which also include non-coding RNAs, with a conserved core motif of G(m^{6}A)C. We further establish the role of YTHDF2 in RNA metabolism, showing that binding of YTHDF2 results in the localization of bound mRNA from the translatable pool to mRNA decay sites, such as processing bodies[9]. The C-terminal domain of YTHDF2 selectively binds to m^{6}A-containing mRNA whereas the N-terminal domain is responsible for the localization of the YTHDF2-mRNA complex to cellular RNA decay sites. Our results indicate that the dynamic m^{6}A modification is recognized by selective-binding proteins to affect the translation status and lifetime of mRNA.

Users may view, print, copy, download and text and data- mine the content in such documents, for the purposes of academic research, subject always to the full Conditions of use: http://www.nature.com/authors/editorial_policies/license.html#terms

*To whom correspondence should be addressed. chuanhe@uchicago.edu.

Supplementary Information is available in the online version of the paper.

Author Contributions C. H. conceived the project. X. W. designed and performed most experiments. Z. L. and X. W. performed data analyses of high-throughput sequencing data. A. G. assisted with the experiments. Y. Y. and D. H. conducted the experimental and data analysis part of m^{6}A profiling, respectively. Y. F. performed the RNA-affinity pull-down experiment of YTHDF1 and YTHDF3. M. P. and G. J. provided valuable discussions. G. H. and B. R. performed high throughput sequencing. Q. D. assisted in m^{6}A synthesis. X. W. and C. H. interpreted the results and wrote the manuscript with input from T. P.

RNA sequencing data were deposited in the Gene Expression Omnibus (http://www.ncbi.nlm.nih.gov/geo) under accession number GSE49339 and the processed results were presented as Supplementary Table 1.

The authors declare no competing financial interests.

Author Manuscript Author Manuscript Author Manuscript Author Manuscript

Messenger RNA (mRNA) is central to the flow of genetic information. Regulatory elements (e.g. AU-rich element, iron-responsive element), in the form of short sequence or structural motif imprinted in mRNA, are known to control the time and location of translation and degradation processes[10]. Reversible and dynamic methylation of mRNA could add another layer of more sophisticated regulation to the primary sequence[2,11]. m^{6}A, a prevalent internal modification in the messenger RNA of all eukaryotes, is post-transcriptionally installed by m^{6}A methyltransferase (e.g., MT-A70, Fig. 1a) within the consensus sequence of G(m^{6}A)C (70%) or A(m^{6}A)C (30%)[12]. The loss of MT-A70 leads to apoptosis in human HeLa cells[13], and significantly impairs development in Arabidopsis[4] and in Drosophila[5]. Our recent discoveries of m^{6}A demethylases FTO (fat mass and obesity-associated protein)[7] and ALKBH5[8] demonstrate that this RNA methylation is reversible and may dynamically control mRNA metabolism. The recently revealed m^{6}A transcriptomes (methylome) in human cells and mouse tissues showed m^{6}A enrichments within long exons and around stop codon[14,15], further suggesting fundamental regulatory roles of m^{6}A. However, despite these progresses the exact function of m^{6}A remains to be elucidated.

While methyltransferase may serve as the “writer” and demethylases (FTO and ALKBH5) act as the “eraser” of m^{6}A on mRNA, potential m^{6}A-selective-binding proteins could represent the “reader” of the m^{6}A modification and exert regulatory functions through selective recognition of methylated RNA. Here, we show that the YTH-domain family member 2 (YTHDF2), initially found in pull-down experiments using m^{6}A-containing RNA probes[14], selectively binds m^{6}A-methylated mRNA and controls RNA decay in a methylation-dependent manner .

The YTH domain family is widespread in eukaryotes and known to bind single-stranded RNA (ssRNA) with the conserved YTH domain (>60% identity) located at the C-terminus[16,17]. In addition to previously reported YTHDF2 and YTHDF3[14], we also discovered YTHDF1 as another m^{6}A-selective binding protein by using methylated RNA bait containing the known consensus sites of G(m^{6}A)C and A(m^{6}A)C versus unmethylated control (Extended Data Fig. 1a). Further, highly purified poly(A)-tailed RNAs were incubated with recombinant GST-tagged YTHDF1–3 and then separated by GST-affinity column. By using a previously reported LC-MS/MS method[7,8], we found that the m^{6}A-containing RNAs were greatly enriched in the YTHDF-bound portion and diminished in the flow-through portion (Fig. 1b, Extended Data Fig. 1b). Gel shift assay revealed that YTHDF2 exhibits a 16-fold higher binding affinity to methylated probe compared to the unmethylated one as well as a slight preference to the consensus sequence (Extended Data Fig. 1c–d). This protein was selected for subsequent characterization since it exhibits a high selectivity to m^{6}A, and was thought to be associated with human longevity[18].

We next applied two independent methods to identify RNAs that are the binding partners of YTHDF2: i) photoactivatable ribounucleoside crosslinking and immunoprecipitation (PAR-CLIP)[19] to locate the binding sites of YTHDF2; ii) sequencing profiling of the RNA of immuno-purified ribonucleoprotein complex (RNP) (RIP-seq)[20] to extract cellular YTHDF2-RNA complexes. Approximately ten thousand crosslinked clusters covering 3,251 genes were identified in PAR-CLIP (Extended Data Fig. 2a–b). Most are mRNA but also 1% belongs to non-coding RNA. Among 2,536 transcripts identified in RIP-seq, 50%

Author Manuscript Author Manuscript Author Manuscript Author Manuscript

overlap with PAR-CLIP targets (Extended Data Fig. 2b). We also performed m^{6}A-seq for the poly(A)-tailed RNA from the same HeLa cell line and found that 59% (7,345, out of 12,442) of the PAR-CLIP peaks of YTHDF2 overlap with m^{6}A peaks (Fig. 1c). As shown in Fig. 1d, the conserved motif revealed from the top 1,000 scored clusters matches the m^{6}A consensus sequence of RRACH[12,14], which strongly supports the binding of m^{6}A by YTHDF2 inside cells (see more motifs in Extended Data Fig. 2c–e). Coinciding with the previously reported pattern of m^{6}A peaks[14,15], YTHDF2 PAR-CLIP peaks showed enrichment near the stop codon and in long exons (Extended Data Fig. 2f–h). YTHDF2 predominantly targets the stop codon region, the 3' untranslated region (3UTR), and the coding region (CDS) (Fig. 1e), suggesting that YTHDF2 may play a role in mRNA stability and/or translation.

To dissect the role of YTHDF2 we employed ribosome profiling to assess the ribosome loading of each mRNA represented as ribosome-protected reads[21,22]. HeLa cells that were treated with YTHDF2 siRNA (Extended Data Fig. 3a) as well as siRNA control were subsequently subjected to ribosome profiling with mRNA-seq performed on the same sample. Transcripts present (RPKM > 1, reads per kilobase, per million reads) in both ribosome profiling and mRNA-seq samples were analyzed. These transcripts were then categorized as YTHDF2 PAR-CLIP targets (3,251), common targets of PAR-CLIP and RIP (1,277), and non-targets (3,905, absent from PAR-CLIP and RIP). A significant increase of input mRNA reads for YTHDF2 targets was observed in the YTHDF2 knockdown sample compared to the control ($p < 0.001$, Mann-Whitney U test), without a noticeable change for non-targets (Fig. 2a). However, compared with the increase in mRNA level, the differences in the ribosome-protected fraction in the knockdown sample compared to the control were small (Fig. 2b). Thus, YTHDF2 knockdown led to apparently reduced translation efficiency of its targets as a result of accumulation of non-translating mRNA (Extended Data Fig. 3b), suggesting the primary role of YTHDF2 in RNA degradation.

Next, we performed RNA lifetime profiling by collecting and analyzing RNA-seq data on YTHDF2 knockdown and control samples obtained at different time points after transcription inhibition with actinomycin D. Indeed, YTHDF2 knockdown led to prolonged (~30% in average) lifetimes of its mRNA targets in comparison with non-targets (Fig. 2c). Interestingly, we found that as the number of binding sites increase the stabilization of the RNA targets caused by YTHDF2 knockdown also increase significantly[23]: more than 4 sites > 2~4 sites > 1 sites (Fig. 2d and Extended Data Fig. 3c, Kruskal-Wallis test, $p < 0.0001$); however, transcripts grouped according to binding region show similar fold change indistinguishable in statistical test (Extended Data Fig.3c–d).

Three pools of mRNAs exist in cytoplasm as defined by their engagement in translation[24,25] (Fig. 2e): non-ribosome mRNPs (mRNA-protein particles, with sedimentation coefficients of 20–35S in sucrose gradient), translatable mRNA pool associated with ribosomal subunits (40–80S), and actively translating polysome (>80S). YTHDF2 was observed to be present in non-ribosome fraction (Fig. 2e). After YTHDF2 knockdown, a 21% increase of the m^{6}A/A ratio of the total mRNA was observed (Fig. 2f), confirming that the presence of YTHDF2 destabilizes the m^{6}A-containing mRNA. YTHDF2 could affect localizing m^{6}A-containing mRNA from a translatable pool to mRNPs. If so, the amount of methylated mRNA should

Author Manuscript Author Manuscript Author Manuscript Author Manuscript

decrease in mRNPs and increase in the translatable pool upon YTHDF2 knockdown. Indeed, after YTHDF2 knockdown, the m^6A/A ratio of mRNA isolated from mRNPs showed a 24% decrease and the ratio from the translatable pool demonstrated a 46% increase (Fig. 2f). We also observed a 14% increase of the m^6A/A ratio of mRNA isolated from polysome after YTHDF2 knockdown (Fig. 2f), although it is worth noting that this model provided no prediction of the behavior of polysome since the ribosome-loading number per transcript depends on the availability of both mRNA and free ribosomes. It should be also noted that the observed m^6A/A ratio change does not appear to be resulted from the protein level change of methyltransferase and demethylase as detected by western blotting (Extended Data Fig. 3e).

Three YTHDF2-targeted RNAs were selected for further validation: the *SON* mRNA has multiple CLIP peaks in CDS, the *CREBBP* mRNA has CLIP peaks at 3'UTR, and a non-coding RNA *PLAC2* (Extended Data Fig. 4a–d). As detected by gene-specific RT-PCR, after 48 h YTHDF2 knockdown, all three RNA transcripts increased by more than 60% with prolonged lifetime; both *SON* and *CREBBP* showed redistribution from non-ribosome mRNP to translatable pool (Extended Data Fig. 4e–n). Furthermore, knockdown of the known m^6A methyltransferase *MT-A70* led to noticeably reduced binding of YTHDF2 to its targets and increased stability of the targets similar to that of the YTHDF2 knockdown (Extended Data Fig. 5).

To gain mechanistic understanding of the YTHDF2-mRNA interaction, we analyzed the cellular distribution of YTHDF2 and found that YTHDF2 co-localizes with three markers (DCP1a, GW182 and DDX6) of processing bodies (P bodies) in cytoplasm, where mRNA decay occurs (Extended Data Fig. 6a–j)[9,26]. YTHDF2 is composed of a C-terminal RNA-binding domain (C-YTHDF2) and a P/Q/N rich N-terminus (N-YTHDF2, Fig. 3a and Extended Data Fig. 6k)[27,28]. While over-expression of YTHDF2 led to a reduced m^6A/A ratio of the total mRNA, over-expression of either N-YTHDF2 or C-YTHDF2 yielded an increased m^6A/A ratio (Fig. 3b), indicating that both domains are required for the YTHDF2-mediated mRNA decay. The *in vitro* pull-down experiment further showed that purified C-YTHDF2 is able to enrich m^6A-containing mRNA from total mRNA (Extended Data Fig. 6l). The spatial distribution of the *SON* mRNA relative to YTHDF2 and N- and C-YTHDF2 truncates were examined by fluorescence *in situ* hybridization (FISH) and fluorescence immunostaining in HeLa cells (Fig. 3c–e). The location of the *SON* mRNA showed a strong correlation with that of the full-length YTHDF2 (Fig. 3c) and C-YTHDF2 (Fig. 3e). In contrast, a much lower correlation was observed for the *SON* mRNA with N-YTHDF2 (Fig. 3d). In addition, the full-length YTHDF2 and N-YTHDF2 co-localized with DCP1a, but to a much less extent for C-YTHDF2, thereby indicating the role of N-YTHDF2 in P-body localization. Furthermore, the over-expression of C-YTHDF2 led to a reduced co-localization of the *SON* mRNA with DCP1a (Fig. 3e).

In further support of this mechanism, N-YTHDF2 was fused with λ peptide (N-YTHDF2-λ) which recognizes Box B RNA with a high affinity in a tether reporter assay[29,30]. Tethering N-YTHDF2-λ to F-luc-5BoxB (five Box B sequence was inserted into the 3UTR of the mRNA reporter) led to a significantly reduced mRNA level (Fig. 3f) and shortening (40%) of its lifetime compared with tethering controls of N-YTHDF2 or λ alone (Extended Data

Author Manuscript Author Manuscript Author Manuscript Author Manuscript

Fig. 7a–e). The reporter mRNA bound by N-YTHDF2-λ possesses shorter poly(A) tail length in comparison with unbound portion, although a significant change of the deadenylation rate was not observed(Extended Data Fig. 7f–l). Together with the observation that YTHDF2 co-localizes with both deadenylation and decapping enzyme complexes (Extended Data Fig. 6), we propose a model (Fig. 3g) that consists of: (1) C-YTHDF2 selectively recognizes m^6A-containing mRNA less engaged with translation; (2) this binding of YTHDF2 to methylated mRNA happens in parallel or at a later stage of deadenylation; (3) N-YTHDF2 localizes the YTHDF2-m^6A-mRNA complex to more specialized mRNA decay machineries (P bodies etc.) for committed degradation.

Functional clustering of YTHDF2 targets versus non-targets revealed that the main functions of YTHDF2-mediated RNA processing are gene expression (molecular function) as well as cell death and survival (cellular function, Extended Data Fig. 8a–d). After 72 hours of YTHDF2 knockdown, the viability of HeLa cells reduced by 50% (Extended Data Fig. 8e–f), indicating that the YTHDF2-mediated RNA processing could have biological significance.

In summary, we present here a transcriptome-wide identification of YTHDF2-RNA interaction and a mechanistic model for m^6A function mediated by this m^6A-binding protein, as the first functional demonstration of a m^6A reader protein. We show that YTHDF2 alters the distribution of the cytoplasmic states of several thousand m^6A-containing mRNA. This present work demonstrates that reversible m^6A deposition could dynamically tune the stability and localization of the target RNAs through m^6A “readers”.

Methods

Plasmid construction and protein expression

Recombinant YTHDF1–3 were cloned from commercial cDNA clones (Open Biosystems) into vector pGEX-4T-1. The primers used for subcloning (from 5’ to 3’; F stands for forward primer; R stands for reverse primer) are listed below:

GST-YTHDF1-F:	CGATCGAATTCATGTCGGCCACCAGCG
GST-YTHDF1-R:	CCATACTCGAGTCATTGTTTGTTTCGACTCTGCC
GST-YTHDF2-F:	CGTACGGATCCATGTCAGATTCCTACTTACCCAG
GST-YTHDF2-R:	CGATGCTCGAGTCATTTCCCACGACCTTGACG
GST-YTHDF3-F:	CGTACGGATCCATGTCAGCCACTAGCGTG
GST-YTHDF3-R:	CGTAGCTCGAGTCATTGTTTGTTTCTATTTCTCTCCCTAC

The resulting clones were transfected into the *E. coli* strain BL21 and expression was induced at 16°C with 1 mM IPTG for 20 h. The pellet collected from 2 L bacteria culture was then lysed in 30 mL PBS-L solution (50 mM NaH_2PO_4, 150 mM NaCl, pH 7.2, 1 mM PMSF, 1 mM DTT, 1 mM EDTA, 0.1% (v/v) Triton X-100) and sonicated for 10 min. After removing cell debris by centrifuge at 12 krpm for 30 min, the supernatant were loaded to GST superflow cartridge (QIAGEN, 5 mL) and gradiently eluted by using PBS-EW (50 mM

Author Manuscript Author Manuscript Author Manuscript Author Manuscript

NaH_2PO_4, 150 mM NaCl, pH 7.2,1 mM DTT, 1 mM EDTA) as buffer A and TNGT (50 mM Tris, pH 8.0, 150 mM NaCl, 50 mM red, GSH, 0.05 % Triton-x-100) as buffer B. The crude products were further purified by gel-filtration chromatography in GF buffer (10 mM Tris, pH 7.5, 200 mM NaCl, 3 mM DTT and 5% glycerol). The yield was around 1–2 mg per liter of bacterial culture.

Flag-tagged YTHDF2 was cloned into vector pcDNA 3.0 (*BamH*I, *Xho*I; forward primer: CGTACGGATCCATGGATTACAAGGACGACGATGACAAGATGTCGGCCAGCAGC C; reverse primer: CGATGCTCGAGTCATTTCCCACGACCTTGACG). Flag-tagged YTHDF2 N-terminal was made by mutating E384 (GAA) to a stop codon (TAA) with Stratagenes QuickChange II site-directed mutagenesis kit (pcDNA-flag-Y2N, forward primer: CTGGATCTACTCCTTCATAACCCCACCCAGTGTTG; reverse primer: CAACACTGG GTGGGGTTATGAAGGAGTAGATCCAG). Flag-tagged YTHDF2 C-terminal was made by cloning amino acids from E384 to the end into vector pcDNA 3.0 (*BamH*I, *Xho*I, forward primer: CGTACGGATCCATGGATTACAAGGACGACGATGACAAGGAACCCCACCC AGTGTT; reverse primer: CGATGCTCGAGTCATTTCCCACGACCTTGACG). Plasmids with high purity for mammalian cell transfection were prepared with a Maxiprep kit (QIAGEN).

Tether reporter: pmirGlo Dual luciferase expression vector (Promega) was used to construct the tether reporter which contains firefly luciferase (F-luc) as the primary reporter and *Renilla* luciferase (R-luc) acting as a control reporter for normalization. F-luc-5BoxB mRNA reporter was obtained by inserting five Box B sequence (5BoxB) into the 3UTR of F-luc (*Sac*I and *Xho*I, the resulting plasmid was named as pmirGlo-5BoxB;). The 5BoxB sequence[29] (see below) was PCR amplified from PRL-5BoxB plasmid which was kindly provided by Prof. Witold Filipowi at Friedrich Miescher Institute for Biomedical Research (forward primer: CGATACGAGCTCTTCCCTAAGTCCAACTACCAAAC; reverse primer: CTATGGCTCGAGATAATATCCTCGATAGGGCCC; sequencing primer: GAC GAGGTG CCTAAAGA)[31].

TTCCCTAAGTCCAACTACTAAACTGGGGATTCCTGGGCCCTGAAGAAGGGCCCC TCGACTAAGTCCAACTACTAAACTGGGCCCTGAAGAAGGGCCCATATAGGGCCC TGAAGAAGGGCCCTATCGAGGATATTATCTCGACTAAGTCCAACTACTAAACTG GGCCCTGAAGAAGGGCCCATATAGGGCCCTGAAGAAGGGCCCTATCGAGGATA TTATCTCGAG

In order to study the decay kinetics of F-luc-5BoxB, another reporter plasmid (pmirGlo-Ptight-5BoxB) was constructed by replacing the original human phosphoglycerate kinase promoter of F-luc with Ptight promoter (restriction sites: *Apa*I and *Bgl*II). Ptight promoter was PCR amplified from pTRE-Tight vector (Clontech; forward primer: CGTACAGATCTCGAGTTTACTCCCTATCAGT; reverse primer: CTGTAGGGCCCT TCTTAATGTTTTTGGCATCTTCCATCTCCAGGCGATCTGACG; sequencing primer: AGCGGTGCGTACAATTAAGG). The resulting plasmid (pmirGlo-Ptight) was subjected to a second round of subcloning by inserting 5BoxB into the 3UTR of F-luc (restriction sites: *Xba*I and *Sbf*I) to generate pmirGlo-Ptight-5BoxB (forward primer:

Author Manuscript Author Manuscript Author Manuscript Author Manuscript

CGATACTCTAGATTCCCTAAGTCCAACTACCAAAC; reverse primer: CTATGGCC TGCAGGATAATATCCTCGATAGGGCCC; sequencing primer: GACGAGGTG CCTAA AGA).

Tether effecter: λ peptide sequence (MDAQTRRRERRAEKQAQWKAAN) was fused to the C-terminal of N-YTHDF2 by subcloning N-YTHDF2 to pcDNA 3.0 with forward primer containing flag-tag sequence and reverse primer containing λ peptide sequence (pcDNA-flag-Y2Nλ, *BamH*I, *Xho*I; forward primer: GATACGGATCCATGG ATTACAAGGACGACGATGACAAGATGTCGGCCAGCAGCC; reverse primer: TAT GGCTCGAGTCAGTTTGCAGCTTTCCATTGAGCTTGTTTCTCAGCGCGACGCTCAC GTCGTCGTGTTTGTGCGTCCATACCTGAAGGAGTAGATCCAGAACC). The λ peptide control was designed with a flag tag at N-terminal and a GGS spacer (pcDNA-flag-λ). The primer pair that contains flag-tagged λ peptide and sticky restriction enzyme sites (*BamH*I, *Xho*I) was annealed and directly ligated to digested pcDNA 3.0 (forward primer: GATCCATGGATTACAAGGACGACGATGACAAGGGTGGTAGCATGGACGCACAA ACACGACGACGTGAGCGTCGCGCTGAGAAACAAGCTCAATGGAAAGCTGCAAA CTAAC; reverse primer: GAGTTAGTTTGCAGCTTTCCATTGAGCTTGTTTCTCAGC GCGACGCTCACGTCGTCGTGTTTGTGCGTCCATGCTACCACCCTTGTCATCGTCG TCCTTGTAATCCATG).

EMSA (Electrophoretic Mobility Shift Assay / Gel shift assay)

The RNA probe was synthesized by a previously reported method with the sequence of 5'-AUGGGCCGUUCAUCUGCUAAAAGGXCUGCUUUUGGGGCUUGU-3'(X = A or m^6A). After the synthesis, the RNA probe was labeled in a reaction mixture of 2 μL RNA probe (1 μM), 5 μL 5×T4 PNK buffer A (Fermentas), 1 μL T4 PNK (Fermentas), 1 μL ^{32}P-ATP and 41 μL RNase-free water (final RNA concentration 40 nM) at 37°C for 1 hour. The mixture was then purified by RNase-free micro bio-spin columns with bio-gel P30 in Tris buffer (BioRad 732–6250) to remove hot ATP and other small molecules. To the elute, 2.5 μL 20 × SSC (Promega) buffer was added. The mixture was heated to 65°C for 10 min to denature the RNA probe, and then slowly cooled down to room temperature. GST-YTHDF1–3 were diluted to concentration series of 200 nmol, 1 μM, 5 μM, 20 μM and 100 μM (or other indicated concentrations) in binding buffer (10 mM HEPES, pH 8.0, 50 mM KCl, 1mM EDTA, 0.05% Triton-X-100, 5% glycerol, 10 μg/mL Salmon DNA, 1 mM DTT and 40 U/mL RNasin). Before loading to each well, 1 μL RNA probe (4 nM final concentration) and 1 μL protein (20 nM, 100 nM, 500 nM, 2 μM, or 10 μM final concentration) were added and the solution was incubated on ice for 30 min. The entire 10 μL RNA-protein mixture was loaded to the gel (Novex 4~20% TBE gel) and run at 4 °C for 90 min at 90 V. Quantification of each band was carried out by using a storage phosphor screen (K-Screen; Fuji film) and Bio-Rad Molecular Imager FX in combination with Quantity One software (Bio-Rad). The *Kd* (dissociation constant) was calculated with nonlinear curve fitting (Function Hyperbl) of Origin 8 software with $y = P_1 \times x/(P_2+x)$, where y is the ratio of [RNA-protein]/[free RNA]+[RNA-protein], x is the concentration of the protein, and P_2 is *Kd*.

Author Manuscript Author Manuscript Author Manuscript Author Manuscript

Mammalian cell culture, siRNA knockdown (KD), and plasmid transfection

Human HeLa cell line used in this study was purchased from ATCC (CCL-2) and grown in DMEM (Gibco, 11965) media supplemented with 10% FBS and 1% 100×Pen Strep (Gibco, 15140). HeLa Tet-off cell line was purchased from Clontech (631156) and grown in DMEM (Gibco, 11965) media supplemented with 10% FBS (Tet system approved, Clontech, 631101), 1% 100×Pen Strep (Gibco, 15140) and 200 μg/mL G418 (Clontech, 631308). *YTHDF2* siRNA was ordered from QIAGEN as custom synthesis which targets 5'-AAGGACGTTCCCAATAGCCAA-3' near the N terminal of CDS. *MT-A70* siRNA was ordered from QIAGEN: 5'-CGTCAGTATCTTGGGCAAGTT-3'. Transfection was achieved by using Lipofectamine RNAiMAX (Invitrogen) for siRNA, and Lipofectamine 2000 for single type of plasmid or Lipofectamine LTX Plus (Invitrogen) for co-transfection of two or multiple types of plasmids (tethering assay) following the manufacturer's protocols.

RNA isolation

mRNA isolation for LC/MSMS: Total RNA was isolated from wild-type or transiently transfected cells with TRIZOL Reagent (Invitrogen). mRNA was extracted using PolyATtract® mRNA Isolation Systems IV (Promega) followed by further removal of contaminated rRNA by using RiboMinus Transcriptome Isolation Kit (Invitrogen). mRNA concentration was measured by NanoDrop. Total RNA isolation for RT-PCR: following the instruction of RNeasy kit (QIAGEN) in addition to DNase I digestion step. Ethanol precipitation: to the RNA solution being purified or concentrated, 1/10 volume of 3 M NaOAc, pH 5.5, 1 μL glycogen (10 mg/mL) and 2.7 volume of 100% ethanol were added, stored at −80 °C for 1 h to overnight, and then centrifuged at 13 krpm for 15 min. After the supernatant was removed, the pellet was washed twice by using 1 mL 75% ethanol, and dissolved in the appropriate amount of RNase-free water as indicated.

In vitro pull down

0.8 μg mRNA (save 0.2 μg from the same sample as **input**) and YTHDF1–3 or C-YTHDF2 (final concentration 500 nM) were diluted into 200 μL IPP buffer (150 mM NaCl, 0.1% NP-40, 10 mM Tris, pH 7.4, 40 U/mL RNase inhibitor, 0.5 mM DTT), and the solution was mixed with rotation at 4 °C for 2 h. For YTHDF1–3, 10 μL GST-affinity magnetic beads (Pierce) were used for each sample after being washed four times with 200 μL IPP buffer for each wash. For C-YTHDF2, 20 μL Dynabeads® His-Tag Isolation & Pulldown beads (Invitrogen) were used after being washed four times with 200 μL IPP buffer for each wash. The beads were then re-suspended in 50 μL IPP buffer. The protein-RNA mixture was combined with GST or His6 beads and kept rotating for another 2 h at 4 °C. The aqueous phase was collected, recovered by ethanol precipitation, dissolved in 15 μL water, and saved as the **flowthrough**. The beads were washed four times with 300 μL IPP buffer each time. 0.4 mL trizol reagent was added to the beads and further purified according to manufacturer's instruction. The purified fraction was dissolved in 15 μL water, and saved as **YTHDF-bound**. LC-MS/MS was used to measure the level of m^6A in each sample of **input**, **flowthrough**, and **YTHDF-bound**.

Author Manuscript Author Manuscript Author Manuscript Author Manuscript

LC-MS/MS[7,8]

200–300 ng of mRNA was digested by nuclease P1 (2 U) in 25 μl of buffer containing 25 mM of NaCl, and 2.5 mM of $ZnCl_2$ at 37 °C for 2 h, followed by the addition of NH_4HCO_3 (1 M, 3 μl) and alkaline phosphatase (0.5 U). After an additional incubation at 37 °C for 2 h, the sample was diluted to 50 μL and filtered (0.22 μm pore size, 4 mm diameter, Millipore), and 5 μl of the solution was injected into LC-MS/MS. Nucleosides were separated by reverse phase ultra-performance liquid chromatography on a C18 column with on-line mass spectrometry detection using Agilent 6410 QQQ triple-quadrupole LC mass spectrometer in positive electrospray ionization mode. The nucleosides were quantified by using the nucleoside to base ion mass transitions of 282 to 150 (m^6A), and 268 to 136 (A). Quantification was performed in comparison with the standard curve obtained from pure nucleoside standards running on the same batch of samples. The ratio of m^6A to A was calculated based on the calibrated concentrations.

m^6A profiling

Total RNA was isolated from HeLa cells with TRIZOL reagent. Poly(A)+ RNA was further enriched from total RNA by using FastTrack MAG Maxi mRNA isolation kit (Invitrogen). In particularly, an additional DNase I digestion step was applied to all the samples to avoid DNA contamination. RNA fragmentation, m^6A-seq, and library preparation were performed according to the previous protocol developed by Dominissini *et al*[14]. The experiment was conducted in two biological replicates (Extended Data Table 1).

RIP-seq

The procedure was adapted from the previous report[20]. 60 million HeLa cells were collected (three 15 cm plates, after 24 h transfection of flag-tagged YTHDF2) by cell lifter (Corning Incorporated), pelleted by centrifuge for 5 min at 1 krcf and washed once with cold PBS (6 mL). The cell pellet was re-suspended with 2 volumes of lysis buffer (150 mM KCl, 10 mM HEPES pH 7.6, 2 mM EDTA, 0.5% NP-40, 0.5 mM DTT, 1:100 protease inhibitor cocktail, 400 U/mL RNase inhibitor; one plate with ~200 μL cell pellet and ~400 μL lysis buffer), pipetted up and down several times, and then the mRNP lysate was incubated on ice for 5 min and shock-frozen at −80°C with liquid nitrogen. The mRNP lysate was thawed on ice and centrifuged at 15 krcf for 15 min to clear the lysate. The lysate was further cleared by filtering through a 0.22 μm membrane syringe. 50 μL cell lysate was saved as **input**, mixed with 1 mL trizol. The anti-flag M2 magnetic beads (Sigma, 20 μL per mL lysate, ~30 μL to each sample) was washed with a 600 μL NT2 buffer (200 mM NaCl, 50 mM HEPES pH 7.6, 2 mM EDTA, 0.05% NP-40, 0.5 mM DTT, 200 U/mL RNase inhibitor) four times and then re-suspended in 800 μL ice-cold NT2 buffer. Cell lysate was mixed with M2 beads; the tube was flicked several times to mix the contents and then rotated continuously at 4 °C for 4 hours. The beads were collected, washed eight times with 1 mL ice-cold NT2 buffer. 5 packed beads volumes (~150 μL = 30 μL×5) of elution solution which was 500 ng/μL 3×Flag peptide (Sigma) in NT2 buffer were added to each sample, and the mixture was rotated at 4°C for 2 hours to elute. The supernatant was mixed with 1 mL trizol and saved as **IP**. RNA recovered from **input** was further subjected to mRNA purification by either Poly(A) selection (replicate 1, FastTrack MAG Maxi mRNA isolation kit, invitrogen) or

Author Manuscript Author Manuscript Author Manuscript Author Manuscript

rRNA removal (replicate 2, RiboMinus Eukaryote Kit v2, Ambion). **Input** mRNA and **IP** with 150–200 ng RNA of each sample were used to generate the library using TruSeq stranded mRNA sample preparation kit (Illumina).

PAR-CLIP

We followed the protocol described by Hafner *et al*. with the following modifications[32]. Sample preparation: Five 15 cm plates of HeLa cells were seeded at Day 1 18:00. At Day 2 10:00, the HeLa cells were transfected with flag-tagged YTHDF2 plasmid at 80% confluency. After six hours, the media was changed and 200 μM 4SU was added. At Day 3 10:00, the media was aspirated, and the cells were washed once with 5 mL ice-cold PBS for each plate. The plates were kept on ice, and the crosslink was carried by 0.15 J/cm^2 Ultraviolet light. 2 mL PBS was added and the cells were collected by cell lifter.

Library construction: The final recovered RNA sample was further cleaned by RNA Clean & Concentrator (Zymo Research) before library construction by Tru-seq small RNA sample preparation kit (Illumina).

Mild enzyme digestion[33]: The first round of T1 digest was carried out under 0.2 U/μL for 15 min instead of 1 U/μL for 15 min. The second round of T1 digest was conducted under 10 U/μL for 8 min instead of 50 U/μL for 15 min.

Ribosome and polysome profiling

The procedure was adapted from the previous report[22]. Eight 15 cm plates of HeLa cells were prepared for 48 h knockdown (siControl, siYTHDF2, four plates each). Before collection, cycloheximide (CHX) was added to the media at 100 μg/mL for 7 min. The media was removed, and the cells were collected by cell lifter with 5 mL cold PBS with CHX (100 μg/mL). The cell suspension was spun at 1.6 krpm for 2 min and the cell pellet was washed once by 5 mL PBS-CHX per plate. 1 mL lysis buffer (10 mM Tris, pH 7.4, 150 mM KCl, 5 mM $MgCl_2$, 100 μg/mL CHX, 0.5% Triton-X-100, freshly add 1:100 protease inhibitor, 40 U/mL SUPERasin) was added to suspend the cells and then kept on ice for 15 min with occasional pipetting and rotating. After centrifuge at 14 krpm for 15 min, the supernatant (~1.2 mL) was collected and tested O.D. at 260 nm (150–200 O.D./mL). To the lysate, 8 μL DNase Turbo was added. The lysate was then split by the ratio of 1:4 (**Portion I: Portion II**). 4 μL Super RNasin was added to Portion I. 40 μL MNase buffer and 3 μL MNase (6000 gel units, NEB) was added to **Portion II**. Both portions were kept at room temperature for 15 min, and then 8 μL SUPERasin was added to **Portion II** to stop the reaction. **Portion I** was saved and mixed with 1 mL Trizol to purify input mRNA. **Portion II** was used for ribosome profiling.

Ribosome profiling: a 10/50% w/v sucrose gradient was prepared in a lysis buffer without Triton-X-100. **Portion II** was loaded onto the sucrose gradient and centrifuged at 4 °C for 4 h at 27.5 krpm. The sample was then fractioned and analyzed by Gradient Station (BioCamp) equipped with ECONO Uv monitor (BioRad) and fraction collector (FC203B, Gilson). The fractions corresponding to 80S monosome (not 40S or 60S) were collected, combined, and mixed with an equal volume of Trizol to purify the RNA. The RNA pellet

Author Manuscript Author Manuscript Author Manuscript Author Manuscript

was dissolved in 30 μL water, mixed with 30 μL 2X TBE-urea loading buffer (Invitrogen), and separated on a 10% TBE-urea gel. A 21 nt and a 42 nt ssRNA oligo were used as size markers, and the gel band between 21 and 42 nt was cut. The gel was passed through a needle hole to break the gel, and 600 μL extraction buffer (300 mM NaOAc, pH 5.5, 1 mM EDTA, 0.1 U/mL RNasin) was added. The gel slurry was heated at 65°C for 10min with shaking, and then filtered through 1 mL QIAGEN filter. RNA was concentrated by ethanol precipitation and finally dissolved in 10 μL of RNase-free water.

Input mRNA: The input RNA was first purified by Trizol and the input mRNA was then separated by PolyATract. The resulting mRNA was concentrated by ethanol precipitation and dissolved in 10 μL of RNase-free water. The mRNA was fragmented by RNA fragmentation kit (Ambion). The reaction was diluted to 20 μL and cleaned up by micro Bio-Spin 30 column (cut-off: 20 bp; exchange buffer to Tris).

Library construction: The end structures of the RNA fragments of ribosome profiling and mRNA input were repaired by T4 PNK: (1) 3' de-phosphorylation: RNA (20 μL) was mixed with 2.5 μL PNK buffer and 1 μL T4 PNK, and kept at 37°C for 1 h; (2) 5'-phosphorylation: to the reaction mixture, 1 μL 10 mM ATP and 1 μL extra T4 PNK were added, and the mixture was kept at 37 °C for 30 min. The RNA was purified by 500 μL Trizol reagent, and finally dissolved in 10 μL water. The library was constructed by Tru-seq small RNA sample preparation kit (Illumina). The sequencing data obtained from ribosome profiling (portion II) were denoted as ribosome-protected fragments and that from RNA input (portion I) as mRNA input. Translation efficiency was defined as the ratio of ribosome-protected fragments and mRNA input, which reflected the relative occupancy of 80S ribosome per mRNA species.

Polysome profiling: sample preparation and sucrose gradient were the same as those of the ribosome profiling procedure except eliminating MNase digestion. The fractions resulting from sucrose gradient were used for western blotting or pooled to isolate total RNA for RT-PCR and mRNA for LC-MS/MS test of m^6A/A ratio.

RNA-seq for mRNA lifetime

Two 10 cm plates of HeLa cells were transfected with YTHDF2 siRNA or control siRNA at 30% confluency. After 6 hours, each 10 cm plate was re-seeded into three 6 cm plates, and each plate was controlled to afford the same amount of cells. After 48 hours, actinomycin D was added to 5 μg/mL at 6 hours, 3 hours, and 0 hours before tripsinization collection. The total RNA was purified by RNeasy kit (QIAGEN). Before construction of the library with Tru-seq mRNA sample preparation kit (Illumina), ERCC RNA spike-in control (ambion) was added to each sample (0.1 μL per sample). Two biological replicates were generated: (1) in replicate 1, RNA spike-in control was added proportional to cell numbers; (2) in replicate 2, RNA spike-in control was added proportional to total RNA. Although data obtained from the two sets showed systematic shift, they led to consistent conclusion that YTHDF2 knockdown leads to prolonged lifetime of its RNA targets (Extended Data Fig. 9).

Author Manuscript Author Manuscript Author Manuscript Author Manuscript

Data analysis of seq-data

General pre-processing of reads: All samples were sequenced by illumine Hiseq2000 with single end 100-bp read length. For libraries that generated from small RNA (PAR-CLIP and ribosome profiling), the adapters was trimmed by using FASTX-Toolkit[34]. The deep sequencing data were mapped to Human genome version hg19 by Tophat version 2.0[35] without any gaps and allowed for at most two mismatches. RIP and Ribosome profiling were analyzed by DESeq[36] to generate RPKM (reads per kilobase, per million reads). mRNA lifetime data were analyzed by Cuffdiff version 2.0[37] to calculate RPKM.

Data analysis for each experiment: (1) for m^{6}A profiling, the m^{6}A-enriched regions in each m^{6}A-IP sample were extracted by using the model-based analysis of ChIP-seq (MACS) peak-calling algorithm[38], with the corresponding m^{6}A-Input sample serving as the input control. For each library, the enriched peaks with p < 1e-5 were used for further analysis; (2) for RIP, enrichment fold was calculated as log_2(IP/input); (3) PAR-CLIP data were analyzed by PARalyzerv1.1 with default settings[39]; (4) for ribosome profiling, only genes with RPKM>1 were used for analysis and the change fold was calculated as log_2(siYTHDF2/siControl); (5) for mRNA lifetime profiling: RKPM were converted to attomole by linear-fitting of the RNA spike-in.

The degradation rate of RNA k was estimated by

$$log_2\left(\frac{A_t}{A_0}\right) = -kt$$

where t is transcription inhibition time (h), A_t and A_0 represent mRNA quantity (attomole) at time t and time 0. Two k values were calculated: time 3 h versus time 0 h, and time 6 h versus time 0 h. The final lifetime was calculated by using the average of k_{3h} and k_{6h}.

$$t_{\frac{1}{2}} = \frac{2}{k_{3h}+k_{6h}}$$

Integrative data analysis and statistics: PAR-CLIP targets were defined as reproducible gene targets among three biological replicates (3,251). RIP targets (2528) were genes with log_2(IP/input) >1. The overlap of PAR-CLIP and RIP targets were defined as CLIP+IP targets (1,277). And non-targets (3,905) should meet the conditions: (1) complementary set of PAR-CLIP targets; (2) RIP enrichment fold <0. For the comparison of PAR-CLIP and m^{6}A peaks, at least 1 bp overlap was applied as the criteria of overlap peaks. Two biological replicates were conducted for ribosome profiling and mRNA lifetime profiling, respectively. And genes with sufficient expression level (RPKM>1) were subjected to further analysis. The change fold that used in the main text is the average of the two log_2(siYTHDF2/siControl) values. Nonparametric Mann-Whitney U test (Wilcoxon rank-sum test, two sided, significance level = 0.05) was applied in ribosome profiling data analysis as previous reported[22]. For the analysis of cell viability (Extended Data Fig.8e), RPF of ribosome profiling data were analyzed by Cuffidff version 2.0 for differential expression test, and the genes that differentially expressed (p<0.05) were subjected to Ingeuity Pathway Analysis

Author Manuscript Author Manuscript Author Manuscript Author Manuscript

(IPA, Ingenuity System). RPF was chosen since it may better reflect the translation status of each gene.

Data accession: All the raw data and processed files have been deposited in the Gene Expression Omnibus (http://www.ncbi.nlm.nih.gov/geo). m^{6}A profiling data are accessible under GSE 46705 (GSM1135030 and GSM1135031 are input samples while GSM1135032 and GSM1135033 are IP samples). All other data are accessible under GSE 49339.

RT-PCR

Real-time PCR (RT-PCR) was performed to assess the relative abundance of mRNA. All RNA templates used for RT-PCR were pre-treated with on column DNase I in the purification step. The RT-PCR primers were designed to span exon-exon junctions in order to further eliminate the amplification of genomic DNA and unspliced mRNA. When the examined gene had more than one isoform, only exon-exon junctions shared by all isoforms were selected to evaluate the overall expression of that gene. RT-PCR was performed by using Platinum one-step kit (Invitrogen) with 200–400 ng total RNA template or 10–20 ng mRNA template. *HPRT1* was used as an internal control because: (1) *HPRT1* mRNA did not have m^{6}A peak from m^{6}A profiling data; (2) *HPRT1* mRNA was not bound by YTHDF2 from the PAR-CLIP and RIP sequencing data; (3) *HPRT1* showed relative invariant expression upon YTHDF2 knockdown from the RNA-seq data; (4) *HPRT1* was a house-keeping gene.

YTHDF2:	TAGCCAACTGCGACACATTC;	CACGACCTTGACGTTCCTTT.
SON:	TGACAGATTTGGATAAGGCTCA;	GCTCCTCCTGACTTTTTAGCAA.
CREBBP:	CTCAGCTGTGACCTCATGGA;	AGGTCGTAGTCCTCGCACAC.
PLAC2:	AAGCGCTACCACATCAAGGT;	CCTCCAACCCAGACTACCTG.
LDLR:	GCTACCCCTCGAGACAGATG;	CACTGTCCGAAGCCTGTTCT.
HPRT1:	TGACACTGGCAAAACAATGCA;	GGTCCTTTTCACCAGCAAGCT.
F-luc or F-luc-5BoxB:	CACCTTCGTGACTTCCCATT;	TGACTGAATCGGACACAAGC.
R-luc:	GTAACGCTGCCTCCAGCTAC;	CCAAGCGGTGAGGTACTTGT.

A combination of knockdown/over-expression/RIP/RT-PCR experiments was conducted to evaluable the occupancy change of YTHDF2 on its RNA targets after MT-A70 (METTL3) knockdown (Extended Data Fig. 5). Two 15 cm plates of HeLa cells were transfected with siControl or siMETTL3 siRNA. After 10 hours, the cells were re-seeded. After 14 hours, the cells were further transfected with flag-tagged YTHDF2 plasmid, and collected after another 24 h (in total 48 h knockdown of METTL3, 24 h o/e of flag-YTHDF2). Anti-flag beads were used to separate YTHDF2-bound portion (IP) from unbound portion (flowthrough) as described in the RIP section.

Fluorescence microscopy

Fluorescent immuno-staining: the protocol of Kedersha *et al*[26] was followed. The cells were grown in an 8-well chamber (Lab-Tek). After treatment indicated in each experiment, the cells were washed once in PBS and then fixed in 4% paraformaldehyde in PBST (PBS with

Author Manuscript Author Manuscript Author Manuscript Author Manuscript

0.05% Tween-20; prepared by mixing paraformalydehyde with PBST, heat at 60 °C until clear, pH~7.5) at r.t. for 15 min under rotating The fixing solution was removed, and −20 °C chilled methanol was immediately added to each chamber and incubated for 10 min at room temperature. The cells were rinsed once in PBS and incubated with blocking solution (10% FBS with PBST) for 1 hour at room temperature under rotation. After that, the blocking solution was replaced with primary antibody (diluted by fold indicated in **Antibodies** section in blocking solution) and incubated for 1 hour at r.t. (or overnight at 4 °C). After being washed 4 times with PBST (300 μL, 5–10 min for each wash), secondary antibody (1:300 dilution in PBST) was added to the mixture and incubated at r.t. for 1 hour. After washing 4 times with PBST (300 μL, 5–10 min for each wash), anti-fade reagent (*slowfade*, invitrogen) was added to mount the slides.

FISH in conjugation with Fluorescent immuno-staining: Stellaris FISH probe with Quasar 570 was used according to the manufacturer's instructions. After the washing step, the sample preparation proceeded to the blocking step of the previous paragraph in the presence of 40 U/mL of RNase inhibitor. Secondary antibodies were Alexa 488 and Alexa 647 conjugates.

Image capture and analysis: The images were captured by Leica SP5 II STED-CW super-resolution laser scanning confocal microscope, analyzed by ImageJ. The colocalization was quantified by JAcoP (ImageJ plug-in) and the Pearson coefficients in main text Figure 3 were gained under Costes' automatic threshold[40].

Protein co-IP

HeLa cells expressing flag-tagged YTHDF2, N-YTHDF2, C-YTHDF2 or pcDNA3.0 blank vector were (three 15 cm plates for each) collected by cell lifter, and pelleted by centrifuge at 1 kpm for 5 min. The cell pellet was re-suspended with 2 volumes of lysis buffer (the same as the one used in RIP), and incubated on ice for 10 min. To remove the cell debris, the lysate solution was centrifuged at 15 krpm for 15 min at 4 °C, and the resulting supernatant was passed through a 0.22 μm membrane syringe filter. While 50 μL of cell lysate was saved as **Input**, the rest was incubated with the anti-flag M2 magnetic beads (Sigma) in ice-cold NT2 buffer (the same as the one used in RIP) for 4 h at 4 °C. Afterwards, the beads was subject to extensive wash with 8 × 1 mL portions of ice-cold NT2 buffer, followed by incubation with the elution solution containing 3×flag peptide (0.5 mg/mL in NT2 buffer, Sigma) at 4 °C for another 2 h. The eluted samples, saved as **IP**, were analyzed by western blotting. For IP samples, each lane was loaded with 2 μg **IP** portion; and the input lane were loaded with 10 μg **Input** portion which corresponded to ~1% of overall input.

Tether assay

Basic setting: 100 ng reporter plasmid (pmirGlo or pmirGlo-5BoxB) and 500 ng effecter plasmid (pcDNA-flag-λ, pcDNA-flag-Y2Nλ, or pcDNA-flag-Y2N) were used to transfect the HeLa cells in each well of six-well plate at 60~80% confluency. After 6 hours, each well was re-seeded into 96-well plate (1:20) and 12-well plate (1:2). After 24 hours, the cells in 96-well plate were assayed by Dual-Glo Luciferase Assay Systems (Promega). *Firefly*

Author Manuscript Author Manuscript Author Manuscript Author Manuscript

luciferase (F-luc) activity was normalized by *Renilla* luciferase (R-luc) to evaluate the translation of reporter. And samples in 12-well plate were processed to extract total RNA (DNase I digested), followed by RT-PCR quantification. The amount of F-luc mRNA was also normalized by that of R-luc mRNA.

RNA IP: Two 15 cm HeLa cells were transfected with 1 μg pmirGlo-5BoxB reporter and 5 μg pcDNA-flag-Y2Nλ effecter plasmids for each plate. After 24 hours, the samples were processed as described in RIP section. The recovered RNA from Input, IP and FT portions were used in poly(A) tail assay.

RNA decay: 200 ng reporter plasmid (pmirGlo-Ptight-5BoxB) and 1 μg effecter plasmid (pcDNA-flag-λ, pcDNA-flag-Y2Nλ, or pcDNA-flag-Y2N) were used for each 6 cm plate to transfect the HeLa Tet-off cell line (Clontech) in the presence of 400 ng doxycycline (Dox, Clontech). The transcription of F-luc5BoxB was under repression at this stage. After 18 hours, the cells in each 6 cm plate were washed twice with PBS, trypsinized, and washed twice with Dox-free media, then splitted to four equal portions and re-seeded to 12-well plate in Dox-free media. After 4 h pulse transcription of F-luc5BoxB, Dox were added to 400 ng in each well. The first time point (t = 0 h) was taken as after 20 minutes[41], then 2h, 4h and 6h. Total RNA extracted from each sample were used for RT-PCR analysis and Poly(A) tail length assay.

Poly(A) tail length assay

Poly(A) tail length assay was performed by using Poly(A) Tail-Length Assay kit (Affymetrix) as previously reported[7]. The protocol of the manufacture (Extended Data Fig. 7f–l) was followed, with 30 cycles of two-step PCR at the last step, and then visualized on 10% non-denaturing TBE gel. The forward primer of F-luc-5BoxB is 5'-CCGCTGAGCAATAACTAGCA-3', and the gene-specific reverse primer is 5'-TGCAATTGTTGTTGTTAACTTGTTT-3'. The forward primer of *CREBBP* mRNA is 5'-GTCTTGGGCAATCCAGATGT-3', and the gene-specific reverse primer is 5'-TTTGAATCCAAGTAGTTTTACCATC -3'.

Antibodies

The antibodies used in this study were listed below in the format of name (application; catalog; supplier; dilution fold): Rabbit anti-YTHDF1 (Western; ab99080; Abcam; 1000). Rabbit anti-YTHDF3 (Western; ab103328; Abcam; 1000). Mouse anti-Flag HRP conjugate (Western; A5892; Sigma; 5000). Rabbit anti-MT-A70 (Western; 15073-1-AP; Proteintech Group; 3000). Rabbit anti-FTO(Western; 5325-1; Epitomics; 10000). Goat anti-GAPDH HRP conjugate (Western; A00192; GeneScript; 15000). Rabbit anti-DCP2 (Western; Ab28658; Abcam; 1000). Rabbit anti-m^{6}A (m^{6}A-seq; 202003; Synaptic Systems; 4 μg/per seq). Rat anti-Flag (IF; 637304; Biolegend; 300). Mouse anti-DCP1a (IF; WH0055802M6; Sigma; 300). Mouse anti-GW182 (4B6) (IF; ab70522; Abcam; 100). Rabbit anti-DDX6 (IF; a300–461A; Bethyl Lab; 250). Anti-HuR (IF; WH0001994M2; Sigma; 50). Goat anti-eIF3 (N-20) (IF; sc-16377; Santa Cruz Biotech; 100). Mouse anti-CNOT7 (IF; sc-101009; Stanta Cruz Biotech; 100). Goat anti-PAN2 (C-20) (IF; sc-82110; Santa Cruz Biotech.; 100). Anti-PARN (IF; ab27778; Abcam; 100). Donkey anti-rat Alexa 488 (IF; A21208; Molecular

Author Manuscript Author Manuscript Author Manuscript Author Manuscript

Probes; 300). Goat anti-rabbit Alexa 647 (IF; A21446; Molecular Probes; 300). Goat anti-mouse Alexa 647 (IF; A21236; Molecular Probes; 300). Donkey anti-goat Alexa 647 (IF; A21447; Molecular Probes; 300).

Supplementary Material

Refer to Web version on PubMed Central for supplementary material.

Acknowledgements

This work is supported by National Institutes of Health GM071440 (C.H.) and EUREKA GM088599 (T.P. and C.H). The Mass Spectrometry Facility of the University of Chicago is funded by National Science Foundation (CHE-1048528). We thank Drs. A. E. Kulozik, W. Filipowicz, and J. A. Steitz for generously providing the sequence and plasmids of the tether reporter. We also thank S. F. Reichard for editing the manuscript.

References

1. Tuck MT. The formation of internal 6-methyladenine residues in eucaryotic messenger RNA. Int. J. Biochem. 1992; 24:379–386. [PubMed: 1551452]
2. Jia G, Fu Y, He C. Reversible RNA adenosine methylation in biological regulation. Trends Genet. 2013; 29:108–115. [PubMed: 23218460]
3. Clancy MJ, Shambaugh ME, Timpte CS, Bokar JA. Induction of sporulation in *Saccharomyces cerevisiae* leads to the formation of N^6-methyladenosine in mRNA: a potential mechanism for the activity of the IME4 gene. Nucleic Acids Res. 2002; 30:4509–4518. [PubMed: 12384598]
4. Zhong S, et al. MTA is an *Arabidopsis* messenger RNA adenosine methylase and interacts with a homolog of a sex-specific splicing factor. Plant Cell. 2008; 20:1278–1288. [PubMed: 18505803]
5. Hongay CF, Orr-Weaver TL. *Drosophila* inducer of MEiosis 4 (IME4) is required for Notch signaling during oogenesis. Proc. Natl. Acad. Sci. USA. 2011; 108:14855–14860. [PubMed: 21873203]
6. Frayling TM, et al. A common variant in the *FTO* gene is associated with body mass index and predisposes to childhood and adult obesity. Science. 2007; 316:889–894. [PubMed: 17434869]
7. Jia G, et al. N^6-methyladenosine in nuclear RNA is a major substrate of the obesity-associated FTO. Nat. Chem. Biol. 2011; 7:885–887. [PubMed: 22002720]
8. Zheng G, et al. ALKBH5 is a mammalian RNA demethylase that impacts RNA metabolism and mouse fertility. Mol. Cell. 2012; 49:18–29. [PubMed: 23177736]
9. Sheth U, Parker R. Decapping and decay of messenger RNA occur in cytoplasmic processing bodies. Science. 2003; 300:805–808. [PubMed: 12730603]
10. Dandekar, T. RNA Motifs and Regulatory Elements. 2 ed.. Berlin Heidelberg: Springer-Verlag; 2002. p. 1-11.
11. He C. Grand challenge commentary: RNA epigenetics? Nature Chem. Biol. 2010; 6:863–865. [PubMed: 21079590]
12. Wei CM, Moss B. Nucleotide sequences at the N^6-methyladenosine sites of HeLa cell messenger ribonucleic acid. Biochemistry. 1977; 16:1672–1676. [PubMed: 856255]
13. Bokar JA, Shambaugh ME, Polayes D, Matera AG, Rottman FM. Purification and cDNA cloning of the AdoMet-binding subunit of the human mRNA (N^6-adenosine)-methyltransferase. RNA. 1997; 3:1233–1247. [PubMed: 9409616]
14. Dominissini D, et al. Topology of the human and mouse m^6A RNA methylomes revealed by m^6A-seq. Nature. 2012; 485:201–206. [PubMed: 22575960]
15. Meyer KD, et al. Comprehensive analysis of mRNA methylation reveals enrichment in 3' UTRs and near stop codons. Cell. 2012; 149:1635–1646. [PubMed: 22608085]
16. Stoilov P, Rafalska I, Stamm S. YTH: a new domain in nuclear proteins. Trends Biochem. Sci. 2002; 27:495–497. [PubMed: 12368078]

Author Manuscript Author Manuscript Author Manuscript Author Manuscript

17. Zhang Z, et al. The YTH domain is a novel RNA binding domain. J. Biol. Chem. 2010; 285:14701–14710. [PubMed: 20167602]
18. Cardelli M, et al. A polymorphism of the YTHDF2 gene (1p35) located in an Alu-rich genomic domain is associated with human longevity. J. Gerontol. A Biol. Sci. Med. Sci. 2006; 61:547–556. [PubMed: 16799135]
19. Hafner M, et al. Transcriptome-wide identification of RNA-binding protein and microRNA target sites by PAR-CLIP. Cell. 2010; 141:129–141. [PubMed: 20371350]
20. Peritz T, et al. Immunoprecipitation of mRNA-protein complexes. Nat. Protoc. 2006; 1:577–580. [PubMed: 17406284]
21. Ingolia NT, Ghaemmaghami S, Newman JR, Weissman JS. Genome-wide analysis *in vivo* of translation with nucleotide resolution using ribosome profiling. Science. 2009; 324:218–223. [PubMed: 19213877]
22. Bazzini AA, Lee MT, Giraldez AJ. Ribosome profiling shows that miR-430 reduces translation before causing mRNA decay in zebrafish. Science. 2012; 336:233–237. [PubMed: 22422859]
23. Mukherjee N, et al. Integrative regulatory mapping indicates that the RNA-binding protein HuR couples pre-mRNA processing and mRNA stability. Mol. Cell. 2011; 43:327–339. [PubMed: 21723170]
24. Huang, R.; Brown, CY.; Morris, DR. mRNA Formation and Function. New York: Academic press; 1997. Chapter 16 Analysis of ribosome loading onto mRNA species: implications for translational control.
25. Shenton D, et al. Global translational responses to oxidative stress impact upon multiple levels of protein synthesis. J. Biol. Chem. 2006; 281:29011–29021. [PubMed: 16849329]
26. Kedersha N, Anderson P. Mammalian stress granules and processing bodies. Methods Enzymol. 2007; 431:61–81. [PubMed: 17923231]
27. Reijns MA, Alexander RD, Spiller MP, Beggs JD. A role for Q/N-rich aggregation-prone regions in P-body localization. J. Cell Sci. 2008; 121:2463–2472. [PubMed: 18611963]
28. Kato M, et al. Cell-free formation of RNA granules: low complexity sequence domains form dynamic fibers within hydrogels. Cell. 2012; 149:753–767. [PubMed: 22579281]
29. Gehring NH, Neu-Yilik G, Schell T, Hentze MW, Kulozik AE. Y14 and hUpf3b form an NMD-activating complex. Mol. Cell. 2003; 11:939–949. [PubMed: 12718880]
30. Behm-Ansmant I, et al. mRNA degradation by miRNAs and GW182 requires both CCR4:NOT deadenylase and DCP1:DCP2 decapping complexes. Genes Dev. 2006; 20:1885–1898. [PubMed: 16815998]
31. Pillai RS, Artus CG, Filipowicz W. Tethering of human Ago proteins to mRNA mimics the miRNA-mediated repression of protein synthesis. RNA. 2004; 10:1518–1525. [PubMed: 15337849]
32. Hafner M, et al. PAR-CliP--a method to identify transcriptome-wide the binding sites of RNA binding proteins. J. Vis. Exp. 2010; (41)
33. Kishore S, et al. A quantitative analysis of CLIP methods for identifying binding sites of RNA-binding proteins. Nature Methods. 2011; 8:559–564. [PubMed: 21572407]
34. Pearson WR, Wood T, Zhang Z, Miller W. Comparison of DNA sequences with protein sequences. Genomics. 1997; 46:24–36. [PubMed: 9403055]
35. Trapnell C, Pachter L, Salzberg SL. TopHat: discovering splice junctions with RNA-Seq. Bioinformatics. 2009; 25:1105–1011. [PubMed: 19289445]
36. Anders S, Huber W. Differential expression analysis for sequence count data. Genome Biol. 2010; 11:R106. [PubMed: 20979621]
37. Trapnell C, et al. Transcript assembly and quantification by RNA-Seq reveals unannotated transcripts and isoform switching during cell differentiation. Nat. Biotechnol. 2010; 28:511–515. [PubMed: 20436464]
38. Zhang Y, et al. Model-based analysis of ChIP-Seq (MACS). Genome Biol. 2008; 9:R137. [PubMed: 18798982]
39. Corcoran DL, et al. PARalyzer: definition of RNA binding sites from PAR-CLIP short-read sequence data. Genome Biol. 2011; 12:R79. [PubMed: 21851591]

Author Manuscript Author Manuscript Author Manuscript Author Manuscript

40. Bolte S, Cordelieres FP. A guided tour into subcellular colocalization analysis in light microscopy. J. Microsc. 2006; 224:213–232. [PubMed: 17210054]

41. Clement SL, Lykke-Andersen J. A tethering approach to study proteins that activate mRNA turnover in human cells. Methods Mol. Biol. 2008; 419:121–133. [PubMed: 18369979]

Author Manuscript Author Manuscript Author Manuscript Author Manuscript

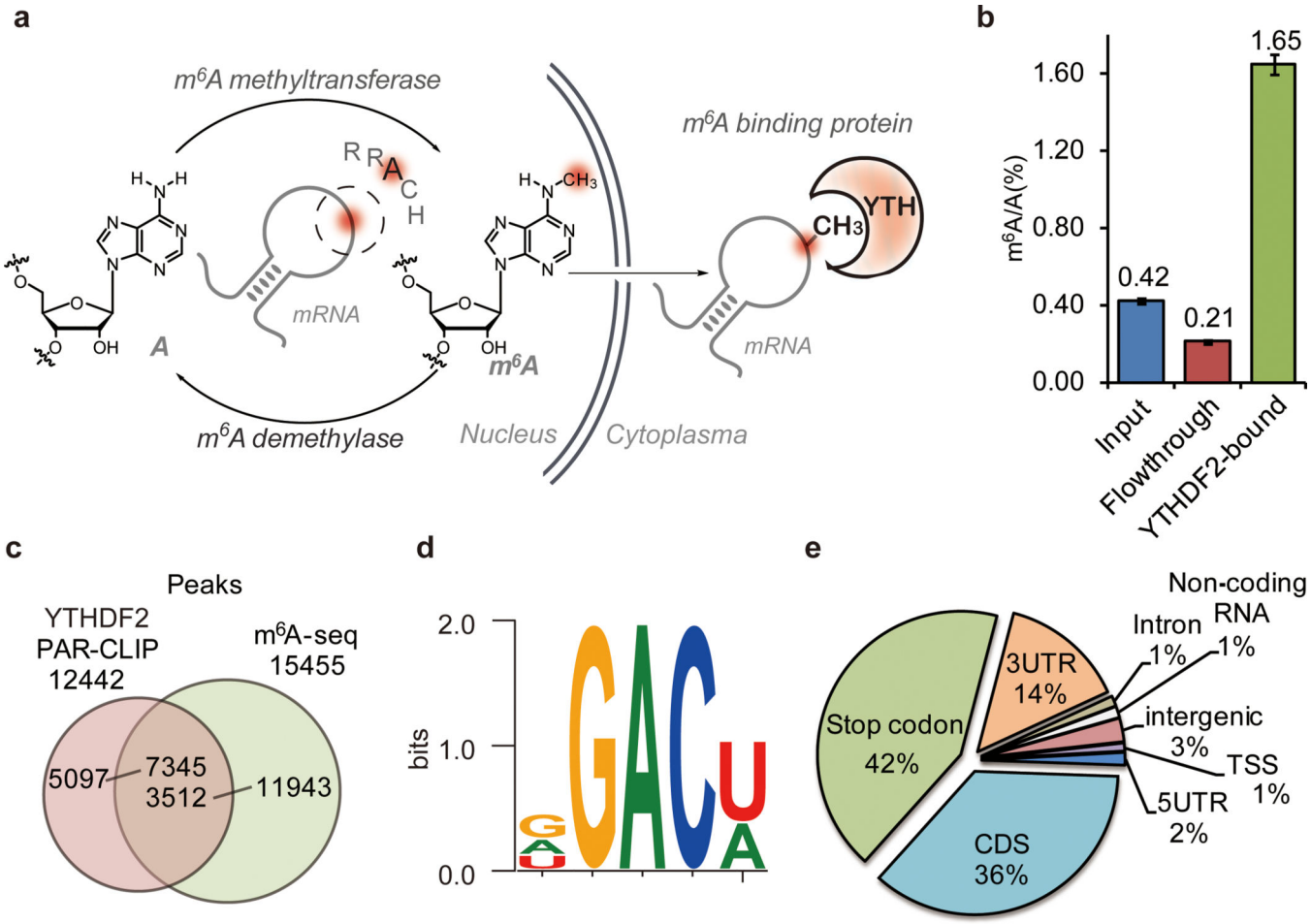

Figure 1. YTHDF2 selectively binds m^{6}A-containing RNA

a, Illustration of m^{6}A methylatransferase, demethylase, and binding proteins. RRACH is the extended m^{6}A consensus motif, where R is G or A and H is not G. **b**, LC-MS/MS showing m^{6}A enrichment in GST-YTHDF2-bound mRNA while depleted in the flow-through portion. Error bars, mean ±s.t.d., n = 2, technical replicates. **c**, Overlap of peaks identified through YTHDF2-based PAR-CLIP and the m^{6}A-seq peaks in the same cell line. **d**, Binding motif identified by MEME with PAR-CLIP peaks (p = 3.0 e−46, 381 sites were found under this motif out of top 1000 scored peaks). **e**, Pie chart depicting the region distribution of YTHDF2-binding sites identified by PAR-CLIP, TTS (200 bp window from the transcription starting site), stop codon (400 bp window centered on stop codon).

Author Manuscript Author Manuscript Author Manuscript Author Manuscript

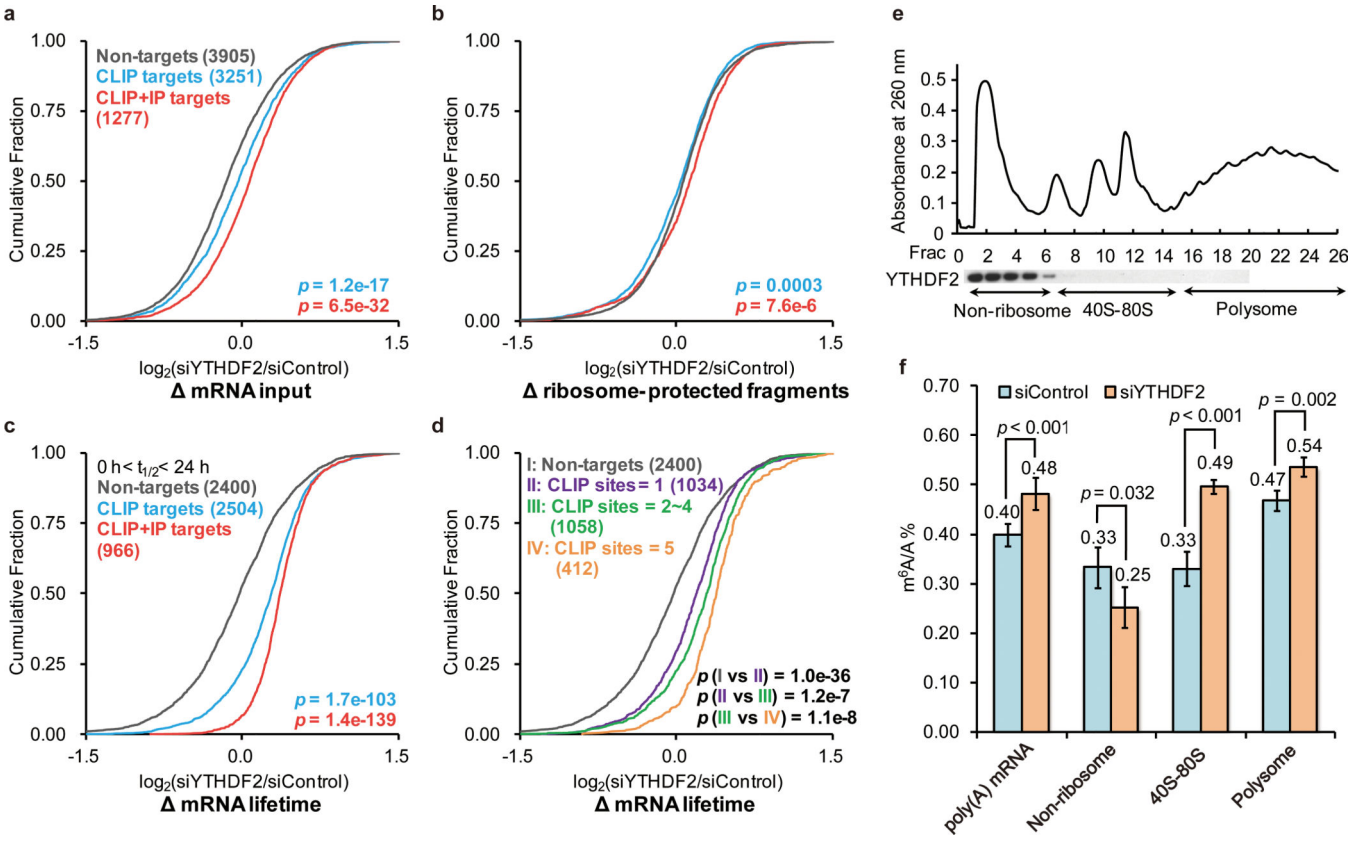

Figure 2. YTHDF2 destabilizes its cognate mRNAs

a–d, Cumulative distribution of mRNA input (**a**), ribosome-protected fragments (**b**), and mRNA lifetime log_2 fold changes (Δ, **c**) between siYTHDF2 (YTHDF2 knockdown) and siControl (knockdown control) for non-targets (grey), PAR-CLIP targets (blue), and PAR CLIP-RIP common targets (red). The mRNA lifetime log_2 fold changes were further grouped and analyzed based on the number of CLIP sites on each transcript (**d**). The increased binding of YTHDF2 on its target transcript correlates with reduced mRNA lifetime. *P* values were calculated using two-sided Mann-Whitney or Kruskal-Wallis test (rank-sum test for the comparison of two or multiple samples, respectively). Detailed statistics were presented in Extended Data Fig. 3c. **e**, Western-blotting of flag-tagged YTHDF2 on each fraction of 10–50% sucrose gradient showing that YTHDF2 does not associate with ribosome. The fractions were grouped to non-ribosome mRNPs, 40–80S, and polysome. **f**, Quantification of the m^6A/A ratio of the total mRNA, non-ribosome portion, 40–80S, and polysome by LC-MS/MS. Noticeable increases of the m^6A/A ratio of the total mRNA, mRNA from 40–80S, and mRNA from polysome were observed in the siYTHDF2 sample compared to control after 48 h. A reduced m^6A/A ratio of mRNA isolated from the non-ribosome portion was observed in the same experiment. *P* values were determined using two-sided Student's *t*-test for paired samples. Error bars, mean ± s.t.d, for poly(A)-tailed total mRNA input, $n = 10$ (five biological replicates × two technical replicates), and for the rest, $n = 4$ (two biological replicates × two technical replicates).

Author Manuscript Author Manuscript Author Manuscript Author Manuscript

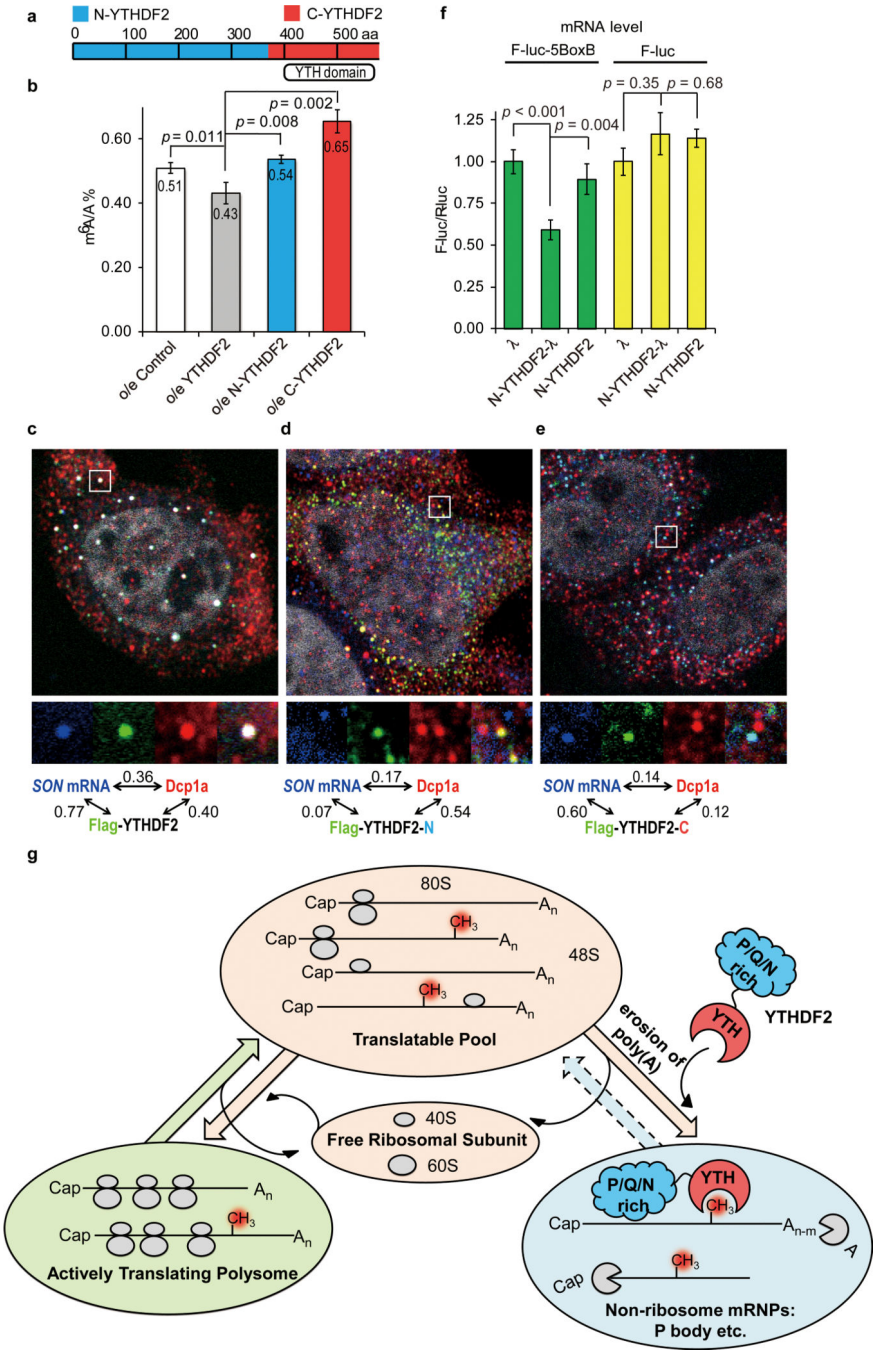

Figure 3. YTHDF2 affects *SON* mRNA localization in processing body (P-body)

a, Schematic of the domain architecture (aa stands for amino acids) of YTHDF2, N-terminal of YTHDF2 (N-YTHDF2, aa 1–389, blue) and C-terminal of YTHDF2 (C-YTHDF2, aa 390-end, red). **b**, Over-expression of full-length YTHDF2 led to reduced levels of m^6A after 24 h, while over-expression of N-YTHDF2 or C-YTHDF2 increased the m^6A/A ratio of the total mRNA. *P* values were determined using two-sided Student's *t*-test for paired samples. Error bars, mean ± s.t.d., $n = 4$ (two biological replicates × two technical replicates). **c**–**e**, Fluorescence *in situ* hybridization of *SON* mRNA and fluorescence immunostaining of

Author Manuscript Author Manuscript Author Manuscript Author Manuscript

DCP1a (P-body marker), flag-tagged YTHDF2 (**c**), flag-tagged C-YTHDF2, (**d**) and flag-tagged N-YTHDF2 (**e**). Full-length YTHDF2 and C-YTHDF2 co-localize with *SON* mRNA (bearing m^6A) while the full-length YTHDF2 significantly increases the P-body localization of *SON* mRNA compared to N-YTHDF2 and C-YTDF2. The numbers shown above figures are Pearson correlation coefficients of each channel pair with the scale of the magnified region (white frame) set as 2 μm × 2 μm. **f**, Tethering N-YTHDF2-λ to a mRNA reporter F-luc-5BoxB led to a ~40% reduction of the reporter mRNA level compared to tethering N-YTHDF2 or λ alone (green) and controls without BoxB (F-luc, yellow). *P* values were determined using two-sided Student's *t*-test for paired samples. Error bars, mean ± s.t.d., n = 6 (F-luc-5BoxB) or 3 (F-luc). **g**, A proposed model of m^6A-dependent mRNA degradation mediated through YTHDF2. The three states of mRNAs in cytoplasm are defined by their engagement with ribosome using the sedimentation coefficient range in sucrose gradient: >80S for actively translating polysome; 40–80S for translatable pool; 20–35S for non-ribosome mRNPs.